

## THE LOCAL HELIOSEISMOLOGY OF INCLINED MAGNETIC FIELDS AND THE SHOWERGLASS EFFECT

H. SCHUNKER,<sup>1</sup> D. C. BRAUN,<sup>2</sup> P. S. CALLY,<sup>1</sup> AND C. LINDSEY<sup>2</sup>

Received 2004 November 18; accepted 2005 February 1; published 2005 February 15

### ABSTRACT

We present evidence for the dependence of helioseismic Doppler signatures in active regions on the line-of-sight angle in inclined magnetic fields. Using data from the Michelson Doppler Imager (MDI) on board the *Solar and Heliospheric Observatory*, we performed phase-sensitive holography in the penumbrae of sunspots over the course of several days as the spots traversed the solar disk. Control correlations, which comprise a correlation of the surface wave amplitude with the incoming acoustic wave amplitude from a surrounding region, were mapped. There is a direct dependence of control-correlation phase signatures on the line-of-sight angle in the plane defined by the vertical and magnetic field vectors. The phase shift of waves observed along directions close to the orientation of the magnetic field is smaller than the phase shift observed when the line of sight is at a significant angle with respect to the field orientation. These findings have important implications for local helioseismology. The variation in phase shift (or the equivalent acoustic travel-time perturbations) with line-of-sight direction suggests that a substantial portion of the phase shift occurs in the photospheric magnetic field. Observations of the vector components of the field may be used to develop a proxy to correct these phase perturbations (known as the acoustic showerglass) that introduce uncertainties in the signatures of acoustic perturbations below the surface.

*Subject headings:* magnetic fields — methods: data analysis — Sun: helioseismology — sunspots

### 1. INTRODUCTION

Considerable progress has been made in recent years in observing and modeling helioseismic signatures of spatially compact sound-speed perturbations and flows in the solar interior. However, various artifacts and biases have been identified as causes for concern in inferences made from observations of  $f$ - and  $p$ -modes observed in the vicinity of photospheric magnetic fields. These include large-amplitude and phase distortions of the wave field due to magnetic fields in the photosphere, known as the “showerglass effect” (Lindsey & Braun 2005a, 2005b), and the effects of  $p$ -mode absorption in sunspots and plage (Braun 1995; Woodard 1997). Helioseismic observations may be corrected for showerglass perturbations, thereby imaging the underlying active region (Lindsey & Braun 2005a). This is based on a strong correlation between the surface magnetic field strength and the phase perturbations. Initial applications of this procedure to data from the Michelson Doppler Imager (MDI; Scherrer et al. 1995) utilize the line-of-sight magnetic field as determined from MDI magnetograms (Lindsey & Braun 2005b).

In this Letter we explore the implications of the surface magnetic field in active regions for helioseismic signals emerging from below the solar surface. Acoustic holography depicts surface oscillations as being caused by upcoming waves from all radial directions and quantifies this in terms of the ingression (§ 2). In the quiet Sun, the ingression and the actual observed surface oscillations correlate well (Lindsey & Braun 2004, 2005a). Our intention is to examine this correlation *inside* active regions, taking particular note of the line-of-sight dependence, with the understanding that the difference between the ingression and the observed surface velocity field is due to photospheric magnetism. This opens up the possibility of both prob-

ing the shallow fields and correcting for their influence when attempting to view deeper structure.

In the presence of a strong surface magnetic field, it is suggested that the fast wave is partially converted to a slow magnetoacoustic mode (which is predominantly acoustic near the surface; Crouch 2003) and is directionally influenced by the magnetic field (Cally et al. 2003; Crouch & Cally 2003). The degree to which this happens is dependent on the inclination of the magnetic field; a uniform field absorbs acoustic energy more efficiently when the acoustic wave propagates at an angle to the magnetic field direction (Cally et al. 2003; Crouch 2003). In addition, inclined fields produce photospheric motion that at any single frequency describes an ellipse whose major axis is tilted toward the inclination angle of the magnetic field (e.g., Fig. 1). The phase for motion along the major axis of the ellipse, for example, lags the phase for motion along the minor axis by 90°.

A consequence of this elliptical motion should be that the phase of the observed magnetoacoustic wave varies with the viewing angle with respect to the field direction. We show how measurements of phase perturbations in sunspot penumbrae observed at various heliocentric angles on the solar disk allow us to confirm and quantify this effect. The properties of the velocity ellipse will depend on the magnetic field amplitude and the tilt of the field relative to the direction of the incident acoustic radiation (Fig. 1).

Using MDI Doppler observations, we examine phase perturbations in the penumbrae of two sunspots, as they rotate across the solar disk. For both sunspots we examine the variation of the observed phase shift with the spatial position within the penumbrae. To determine the phase shift of the waves introduced by the field, the correlation between the incident acoustic wave and the surface velocity is computed using helioseismic holography. Assuming the penumbrae are characterized by axisymmetric-inclined magnetic fields, we expect that the phase shift will depend on the azimuthal angle around the sunspot, with the difference in phase shift being the greatest between locations in the penumbra toward and away from disk

<sup>1</sup> Centre for Stellar and Planetary Astrophysics, School of Mathematical Sciences, Monash University, Clayton, VIC 3800, Australia; hannah.schunker@sci.monash.edu.au, paul.cally@sci.monash.edu.au.

<sup>2</sup> NorthWest Research Associates, Inc., Colorado Research Associates Division, 3380 Mitchell Lane, Boulder, CO 80301; dbraun@cora.nwra.com, clindsey@cora.nwra.com.

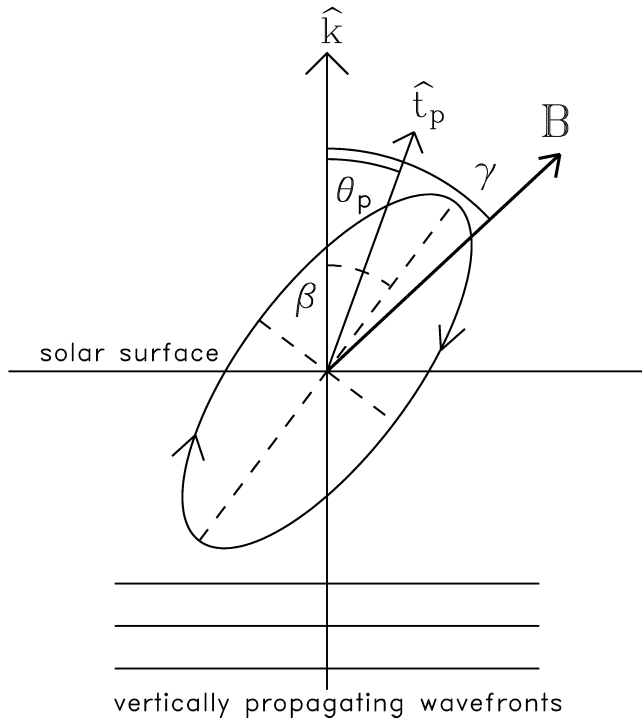


FIG. 1.—Diagram of the effect of an inclined magnetic field on acoustic waves. Upcoming vertical waves impinge on the solar photosphere from below with a direction of propagation,  $\hat{k}$ , normal to the surface;  $\hat{t}_p$  is the projection of the line of sight onto the plane defined by the magnetic field vector,  $\mathbf{B}$ , and  $\hat{k}$ ; and  $\theta_p$  is the angle between  $\hat{t}_p$  and  $\hat{k}$ . The velocity develops a transverse component relative to the vertical as a result of the presence of the inclined magnetic field. The resulting motion is described by an ellipse with a major axis tilted from  $\hat{k}$  by an angle  $\beta$ .

center. For one of the sunspots, vector magnetograph data are also available, and subsequently the orientation and strength of the magnetic field can be directly assessed.

## 2. PROCEDURE

Helioseismic holography reveals subsurface features of the Sun based on the observations of surface velocity (e.g., Lindsey & Braun 2000). The procedure infers the amplitudes of acoustic waves propagating through a focal point located at horizontal position  $\mathbf{r}$  and depth  $z$ . The domain of the focal point (focal plane) is a surface of constant depth. For this study the focal plane is raised to the surface, allowing a comparison of the surface velocities with acoustic waves propagating up to the surface through the interior. The amplitude of incoming waves at position  $\mathbf{r}$ , depth  $z$ , and time  $t$  is called the ingression,

$$H_-(\mathbf{r}, z, t) = \int dt' \times \int_{a < |\mathbf{r}-\mathbf{r}'| < b} d^2\mathbf{r}' G_-(|\mathbf{r}-\mathbf{r}'|, z, t-t')\psi(\mathbf{r}', t), \quad (1)$$

which in this Letter is calculated at  $z = 0$ . The Green's function  $G_-$  represents the subsurface disturbance at  $(\mathbf{r}, z, t)$  resulting from a unit acoustic impulse originating at surface coordinates  $(\mathbf{r}', 0, t')$ . We use a Green's function derived in a wave-mechanical formalism, including effects for disper-

sion (Lindsey & Braun 2004). The computation is confined to an annulus or “pupil” surrounding the focal point  $\mathbf{r}$  with inner and outer radius  $a$  and  $b$ , respectively. The ingression calculated in this way is essentially what *should* result from the incoming acoustic waves propagating from the pupil to the focal point in the absence of perturbations.

To ascertain the effect of a surface anomaly, such as a magnetic field, the ingression is correlated with the surface velocity signal at  $\mathbf{r}$ . In the space-frequency domain, the correlation,

$$C(\nu) = \langle \hat{H}_-(\mathbf{r}, \nu) \hat{\psi}^*(\mathbf{r}, \nu) \rangle_{\Delta\nu}, \quad (2)$$

is an example of a “local control correlation” (Lindsey & Braun 2005a). Here,  $\hat{\psi}$  represents the temporal Fourier transform of the surface disturbance  $\psi$ ,  $\nu$  is the temporal frequency, and  $\hat{H}_-$  represents the temporal Fourier transform of the ingression. The asterisk denotes complex conjugation, and the angle brackets indicate an average over a positive frequency range  $\Delta\nu$  of 1 mHz centered at 5 mHz. The effects of the surface perturbations are quantified by the phase of the correlation,

$$\delta\phi = \arg [C(\nu)]. \quad (3)$$

For the sunspot in Active Region 9026, we used MDI observations spanning 2000 June 3–12 as the spot rotated from a heliographic angular distance of approximately  $60^\circ$  east of the central meridian to about  $60^\circ$  west of the meridian. For the sunspot in AR 9033, we reduced the MDI data obtained between 2000 June 7 and 11.

The full-disk MDI data were analyzed in 24 hr sets. For each day, Postel projections were made, centered near the sunspots. From the temporal Fourier transform, the ingression was computed and correlated to the surface Doppler signal (eqs. [1] and [3]). The pupil size is  $a = 20.7$  Mm and  $b = 43.5$  Mm for the inner and outer radius, respectively. At a frequency of 5 mHz, this pupil selects  $p$ -modes with spherical harmonic degrees ( $\ell$ ) and radial order ( $n$ ) between  $\ell \approx 450$  ( $n = 5$ ) and  $\ell \approx 700$  ( $n = 4$ ). Simple analysis of the acoustic dispersion relation near the surface reveals that  $\cot \eta \approx 2\pi\nu R_\odot / c\ell$ , where  $R_\odot$  is the solar radius,  $\eta$  is the propagation angle from vertical, and  $c$  is the local sound speed. At 5 mHz, and in the given range of  $\ell$ ,  $\cot \eta \approx 10$ , indicating a primarily vertical propagation.

## 3. RESULTS

To identify the existence of a line-of-sight variation in the phase shift, we plot the correlation phase,  $\delta\phi$ , against the azimuthal angle,  $\xi$ , around the penumbra (see Figs. 2 and 3). The inner and outer radii of the penumbrae for both spots were determined from MDI continuum images; these are 7.3–16 Mm for AR 9026 and 10.1–18.9 Mm for AR 9033.

The azimuthal angle is defined as  $\xi = 0^\circ$  toward the west and increases in an anticlockwise direction. Figure 2 shows the correlation phase as a function of  $\xi$  determined within the penumbra of the sunspot in AR 9026 on 3 separate days, as the sunspot rotated across the disk. Figure 3 shows the results obtained in the penumbra of the sunspot in AR 9033 on 2 days. Vertical lines in each panel represent the azimuthal direction toward disk center. The offset of the mean from zero is consistent with previous measurements of the phase of control correlations within the sunspot penumbra near disk center (Lindsey & Braun 2005a), consistent with a travel-time decrease with respect to the quiet Sun.

What is now observed for the first time is a clear cyclic var-

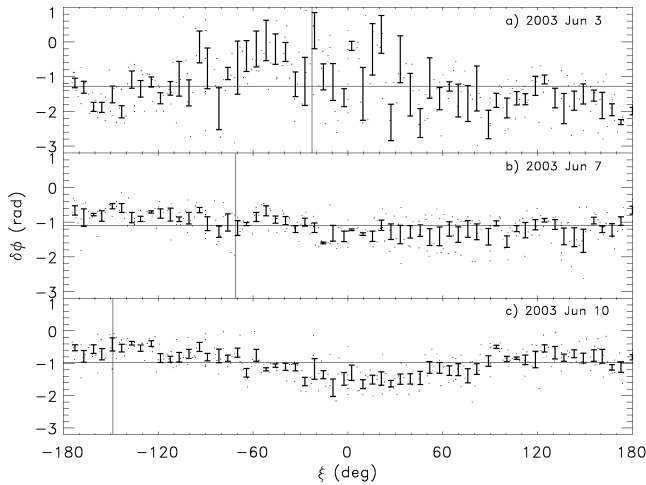


FIG. 2.—Correlation phase,  $\delta\phi$ , in the penumbra of the sunspot in AR 9026 plotted against azimuthal angle  $\xi$  for three positions of the spot: (a) the spot is near the east limb with a heliocentric distance of  $62^\circ$  from disk center, (b) the spot is near the central meridian with a distance of  $21^\circ$  from disk center, and (c) the spot is near the west limb at a distance of  $38^\circ$ . The horizontal lines indicate the mean  $\delta\phi$  averaged over the entire penumbra for each day. The vertical lines indicate the azimuthal direction toward disk center. The error bars represent the standard deviation of the mean over bins of five measurements in  $\xi$ .

iation of the phase shift with azimuthal angle in the penumbrae of both sunspots. Moreover, the variation appears to be related to the direction toward the center of the disk, in the sense that the correlation phase is closest to zero toward disk center, and deviates most substantially away from zero in the direction away from disk center. We interpret this variation of  $\delta\phi$  as caused by a change in the line-of-sight direction with respect to the magnetic field. The cyclic variation is also evident at frequencies of 3 and 4 mHz. With a spreading penumbral magnetic field that is roughly axisymmetric, we assume that when the sunspot is near the limb (Figs. 2a and 2c; Fig. 3a), the line of sight is significantly more aligned with the field in the direction toward disk center than for the direction away from disk center. When the spot is closer to disk center (Figs. 2b and 3b), the variation of the line-of-sight angle with respect to the field lines is more constant with  $\xi$ . This is consistent with observations that show significantly less variation of  $\delta\phi$  with  $\xi$  when the spots are near disk center. Figures 2 and 3 show that the phase of the correlation is heavily dependent on the azimuthal direction around the spot and therefore the angle between the line-of-sight and magnetic azimuths.

Data from the Imaging Vector Magnetograph (IVM) at the University of Hawaii Mees Solar Observatory (Mickey et al. 1996) are available for AR 9026 that provide the orientation and strength of the surface magnetic field in the sunspot. The IVM observations were made during a 28 minute interval starting at 18:29 UT on 2000 June 5. Rotation and scaling were applied to align the IVM data to the line-of-sight MDI magnetogram. The sunspot is shown to have an azimuthally spreading magnetic field but is not entirely symmetric. Figure 4 exhibits the relationship between the magnetic field inclination,  $\gamma$ , and the magnetic field strength in the penumbra of AR 9026. An inverse relationship between inclination and field strength is obvious. From the tight correlation in Figure 4, it is difficult to independently determine the variation of the phase shift with both field strength and inclination. Consequently, we divide the penumbra region into three bins:  $\gamma < 42^\circ$ ,  $42^\circ < \gamma < 66^\circ$ , and

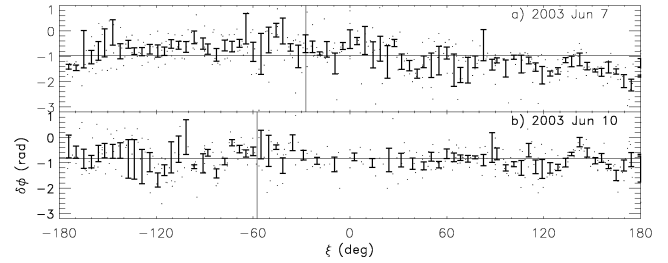


FIG. 3.—Same as in Fig. 2, but for the sunspot in AR 9033 when the spot is (a) near the east limb (with a heliocentric distance of  $60^\circ$ ) and (b) closer to disk center (with a heliocentric distance of  $23^\circ$ ).

$\gamma > 66^\circ$  largely correspond to an increasing distance from the center of the sunspot. The mean magnetic field strengths in the three bins are 1900, 1400, and 600 G, respectively. We have assumed, supported largely by available line-of-sight MDI magnetograms, that there was no significant evolution of the magnetic field in the sunspot in AR 9026 during the 9 days of observations.

We define  $\theta_p$  as the angle of the line-of-sight  $\hat{t}$  from vertical, projected into the plane containing the magnetic field  $\mathbf{B}$  and the vector normal to the photosphere (Fig. 1). We expect that the phase shift between the ingestion and the surface amplitude depends on the magnitude and inclination of the field as well as the projected line-of-sight angle  $\theta_p$ . The full vector magnetic field allows us to study the dependence of the phase shifts on the line-of-sight angle, independent of assumptions of the field symmetry. Figure 5 shows the variation of  $\delta\phi$  with  $\theta_p$  for the three bins of  $\gamma$ , to get a general idea of the behavior with increasing inclination (or magnetic field strength).

There is a significant variation of  $\delta\phi$  with  $\theta_p$ , apparent in Figure 5. There is more scatter in the top panel, suggesting that there is more noise in the correlation for points in higher magnetic field regions (e.g., closer to the sunspot umbrae). However, the variation of  $\delta\phi$  is seen for all inclinations, with the greatest range for the strongest fields. We interpret the variation of the phase in Figure 5 as evidence that the phase shift introduced by inclined magnetic fields depends on the line-of-sight angle, consistent with the concept that the wave

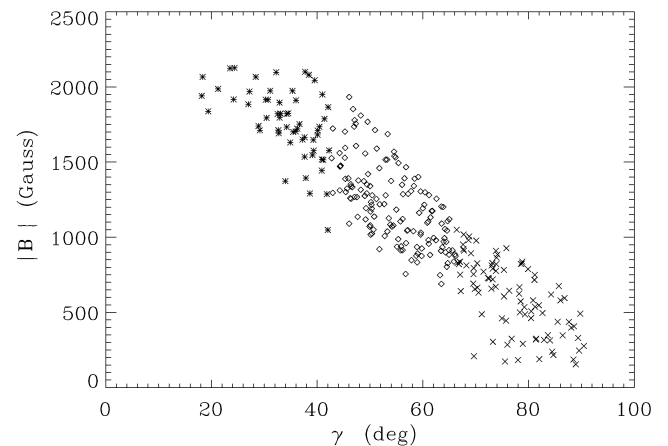


FIG. 4.—Magnetic field strength vs. inclination for the sunspot penumbra in AR 9026 determined from the IVM on 2000 June 5. The different symbols divide the region into three bins of magnetic field inclination:  $\gamma < 42^\circ$  (asterisks),  $42^\circ < \gamma < 66^\circ$  (diamonds), and  $\gamma > 66^\circ$  (mult crosses). In general, the progression from the upper left portion of the distribution to the lower right portion represents an increasing distance from the center of the sunspot.

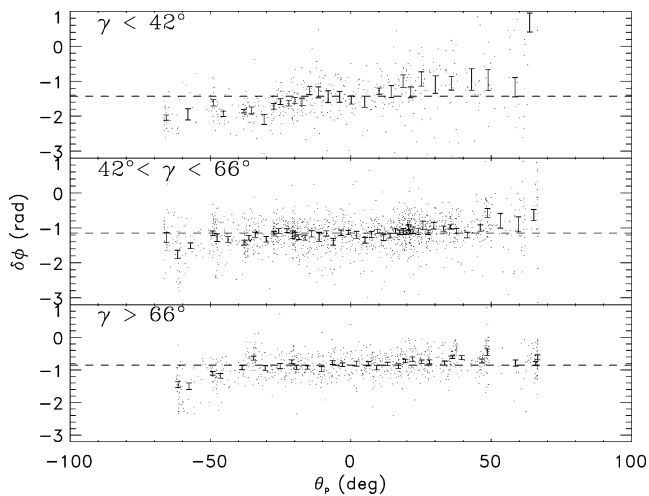


FIG. 5.—Correlation phase ( $\delta\phi$ ) in the penumbra of the sunspot in AR 9026 plotted against projected angle  $\theta_p$  for different values of magnetic field inclinations as indicated. Measurements for the days 2000 June 3–12 are included. The three different panels represent different portions of the penumbra, as shown in Fig. 4. The top panel shows  $\gamma < 42^\circ$ , where the mean field strength  $\langle B \rangle = 1900$  G, the middle panel shows  $42^\circ < \gamma < 66^\circ$ , where  $\langle B \rangle = 1400$  G, and the bottom panel shows  $\gamma > 66^\circ$ , where  $\langle B \rangle = 600$  G. The horizontal dashed lines indicate the mean value of  $\delta\phi$  for each panel. The error bars indicate the standard deviation of the mean over bins of 20 measurements in  $\theta_p$ .

velocity does in fact have a significant component along the direction of the magnetic field vector near the surface. The previous discussion of the variations of  $\delta\phi$  with  $\xi$  shown in Figures 2 and 3 is consistent with this interpretation. For the points plotted in the middle panel of Figure 5, the inclination of the magnetic field is around  $60^\circ$ . Thus, as  $\theta_p$  varies from  $-60^\circ$  to  $+60^\circ$ , we are observing at an angle with respect to the field ranging from  $+120^\circ$  to  $0^\circ$  as we move around the sunspot penumbra.

Local helioseismic measurements at 5 mHz offer the advantage of finer spatial resolution than similar analyses performed with waves at lower temporal frequencies. For several of the MDI data sets discussed above, we repeated the analyses with 1 mHz-wide frequency bandpasses centered at 3 and 4 mHz. The results show a similar variation of the phase of the control correlations with line-of-sight angle. The amplitude of the phase-shift variation appears to scale roughly with temporal frequency. For example, where Figure 2c shows a peak-to-trough amplitude of about 1 radian at a frequency of 5 mHz, the corresponding amplitudes at 3 and 4 mHz are approximately 0.5 and 0.7 radians, respectively.

#### 4. CONCLUSIONS

The results from simple models predict that the upcoming acoustic wave interacts with the magnetic field so that at the surface the velocity vector is somewhat aligned with the magnetic field direction. The correlation phase, which expresses the effect that the magnetic field has had on the incoming wave, clearly varies with  $\xi$  with an amplitude that depends on the heliocentric distance of the sunspot from disk center. The sense is that there is a significantly smaller phase shift when observing along the direction of the magnetic field, compared to when the field is perpendicular to the line of sight. The effect is confirmed by plotting the correlation phase against the projected line-of-sight angle. The strength of the effect is dependent on the magnitude and/or inclination of the magnetic field, there being apparently less variation with  $\theta_p$  for weaker or more inclined fields. The next step is to determine the velocity ellipse of the wave motion from these data and to compare the results with simple models.

These findings have obvious and important implications for understanding and modeling the showerglass effect, and for interpretation of local helioseismic signals around and beneath sunspots, particularly those inferred using observations of the velocity field inside the spots. It is noteworthy that the variation of the phase shifts with viewing angle around sunspot penumbrae, for waves between 3 and 5 mHz, represents an equivalent variation of phase travel times on the order of 30 s. This is comparable to travel-time perturbations inferred from several local helioseismic methods in sunspots that have been interpreted as subsurface variations of sound speeds or flows extending several megameters beneath the photosphere (Kosovichev et al. 2000). However, the existence of variations of the phase shift with the line-of-sight angle suggests a photospheric magnetic origin for much, and perhaps most, of the wave perturbation. Observations of the vector components of the photospheric fields might be used to correct these phase perturbations analogous to the procedures described by Lindsey & Braun (2005a, 2005b). These results certainly suggest that helioseismologists studying the subsurface structure of active regions consider and include details of the magnetic field, including the geometry, in their models.

Many thanks to K. D. Leka for providing the high-quality IVM data provided by the Mees Solar Observatory and to Aaron Birch for useful discussions. D. C. B. and C. L. are supported by the National Aeronautics and Space Administration through the “Living With a Star” and “Sun-Earth Connection” SR&T programs and by the National Science Foundation through the Stellar Astronomy and Astrophysics program.

#### REFERENCES

- Braun, D. C. 1995, *ApJ*, 451, 859  
 Cally, P. S., Crouch, A. D., & Braun, D. C. 2003, *MNRAS*, 346, 381  
 Crouch, A. D. 2003, Ph.D. thesis, Monash Univ.  
 Crouch, A. D., & Cally, P. S. 2003, *Sol. Phys.*, 214, 201  
 Kosovichev, A. G., Duvall, T. L., Jr., & Scherrer, P. H. 2000, *Sol. Phys.*, 192, 159  
 Lindsey, C., & Braun, D. C. 2000, *Sol. Phys.*, 192, 261  
 Lindsey, C., & Braun, D. C. 2004, *ApJS*, 155, 209  
 ———. 2005a, *ApJ*, 620, 1107  
 ———. 2005b, *ApJ*, 620, 1118  
 Mickey, D. L., et al. 1996, *Sol. Phys.*, 168, 229  
 Scherrer, P. H., et al. 1995, *Sol. Phys.*, 162, 129  
 Woodard, M. F. 1997, *ApJ*, 485, 890